Journal of Sound and Vibration (1997) **205**(3), 275–292

AN ANALYTICAL MODEL FOR THE PREDICTION OF THE VIBRATION RESPONSE OF ROLLING ELEMENT BEARINGS DUE TO A LOCALIZED DEFECT

N. TANDON AND A. CHOUDHURY

ITMME Centre, Indian Institute of Technology, Hauz Khas, New Delhi-110016, *India*

(*Received* 6 *February* 1996, *and in final form* 10 *February* 1997)

An analytical model has been proposed for predicting the vibration frequencies of rolling bearings and the amplitudes of significant frequency components due to a localized defect on outer race, inner race or on one of the rolling elements under radial and axial loads. The model predicts a discrete spectrum having peaks at the characteristic defect frequencies and their harmonics. In the case of an inner race defect or a rolling element defect under a radial load, there are sidebands around each peak. The effect of load and pulse shape on the vibration amplitude has been considered in the model. Typical numerical results for a 6002 deep groove ball bearing have been obtained and plotted. A comparison with the experimental values obtained from published literature shows that the model can be successfully used to predict amplitude ratios among various spectral lines.

1. INTRODUCTION

The study of vibration generated by rolling element bearings of a rotating machine is important for condition monitoring and system maintenance. Even geometrically perfect bearings may generate vibration due to varying compliance [1] or due to the time-varying contact forces which exist between the various components of the bearing [2].

However, for condition monitoring it is more important to know the nature of vibration caused by bearing defects, which may be classified into distributed and localized defects. Surface roughness, waviness, misaligned races and off-size rolling elements are included in the class of distributed defects. The localized defects, on the other hand, include cracks, pits and spalls caused by fatigue on the rolling surfaces. When such a defect on one surface strikes its mating surface, a pulse of short duration is produced which excites the natural frequencies of bearing parts and housing structures. For a constant rotational speed, these pulses are generated periodically, and the frequency of pulse generation, termed the "characteristic defect frequency", can be determined uniquely by the location of the defect; whether it is on the inner race, outer race or on one of the rolling elements [3, 4]. Expressions for characteristic defect frequencies for a rolling element bearing with a stationary outer race are shown in Appendix I.

Excitation of the natural frequencies of the bearing elements because of the presence of local defect results in an increase in the vibration energy at these high frequencies (>5 kHz) [3], but the components at the characteristic defect frequencies appear in the low frequency band of the frequency spectrum.

In this paper an analytical model has been developed to predict frequency and amplitude for this low frequency band due to a local defect in a bearing element. It is assumed that

0022–460X/97/330275 + 18 $25.00/0/sv971031

the vibration signal received at the transducer is the vibration of races transmitted through and affected by transmitting media such as the housing, etc. Therefore expressions have been presented here for the amplitude of vibratory displacement of races due to a localized defect taking into account the effects of the load (both radial and axial), the location of the defect and the shape of the generated pulse.

2. GENERATION OF THE MATHEMATICAL MODEL

In order to determine the vibration response, the bearing rings are assumed to be isolated continuous systems. It is further assumed that the outer race remains stationary and that the inner race rotates at the shaft speed.

The natural frequency for the ith mode of flexural vibration of the races can be obtained from the expression [3, 5]

$$\omega_i = \frac{i(i^2-1)}{\sqrt{1+i^2}}\sqrt{\frac{EI}{\rho a^4}}, \tag{1}$$

where i is the number of sine waves around the circumference ($=2, 3, 4, \ldots$), a is the radius of neutral axis, I is the moment of inertia of the cross-section, E is the modulus of elasticity and ρ is the mass per unit length.

The mode summation method [6] as applied by Meyer *et al*. [2] is used here to determine the vibratory response. It is assumed that the deflection pattern of the bearing rings is the sum of sine and cosine waves around the rings.

2.1. EQUATIONS OF MOTION

With the help of Lagrange's equation, we obtain the equation of motion for the outer race as

$$\ddot{q}_{i,\sin} + \omega_i^2 q_{i,\sin} = Q_{i,\sin}/M_i, \qquad \ddot{q}_{i,\cos} + \omega_i^2 q_{i,\cos} = Q_{i,\cos}/M_i, \tag{2}$$

where $q_{i,\sin}$ and $q_{i,\cos}$ are the generalized co-ordinates for the ith sine and cosine modes, $Q_{i,\sin}$ and $Q_{i,\cos}$ are the generalized forces for the ith sine and cosine modes, and M_i and ω_i are the generalized mass and natural frequency for the ith mode.

For the deflection of the inner race, the differential equation can be expressed as

$$\ddot{q}'_{i,\sin} + \omega_i'^2 q'_{i,\sin} = Q'_{i,\sin}/M'_i, \qquad \ddot{q}'_{i,\cos} + \omega_i'^2 q'_{i,\cos} = Q'_{i,\cos}/M'_i, \tag{3}$$

where $q'_{i,\sin}$, $q'_{i,\cos}$, $Q'_{i,\cos}$, $Q'_{i,\sin}$, M'_i and ω'_i denote the corresponding parameters for the inner race.

2.2. GENERALIZED FORCE

In order to obtain the generalized force Q_i, it is to be noted that the external excitation is the pulse generated whenever the defect is struck by rolling elements in the case of a race defect, or the defect on the rolling element strikes the races. The generalized force for a bearing ring may be expressed as

$$Q_i = \int_0^{2\pi} p(\phi, t) X_i(\phi)\, \mathrm{d}\phi, \tag{4}$$

where X_i is the mode shape and $p(\phi, t)$ is the excitation force which is the product of load on the rolling element, P, and the pulse shape, F.

2.2.1. *The ball/roller load*

The magnitude of the generated pulse depends on the ball/roller load, P, at the time of excitation. Therefore, in the case of a stationary defect, P, as well as the magnitude of the pulse, remains constant. However, with a change in defect position, P, as well as the pulse magnitude, may attain a new constant value.

In case of a moving defect (inner race defect or rolling element defect), the load at the point of excitation does not remain constant. Since a rolling element moves at the cage speed ω_c, the load on the rolling element causing excitation due to the moving defect can be expressed as $P(\omega_c t)$.

In the case of pure axial loading, the load on any rolling element at any arbitrary position is constant. Therefore

$$P(\omega_c t) = P_t = \text{constant}.$$

However, for radial loading the load will change with the angular position, as shown in Figure 1. The load on the rolling element at any angle ϕ $(=\omega_c t)$ can be expressed as [7]

$$P(\phi) = \begin{cases} P_{max}[1 - (1/2\varepsilon)(1 - \cos\phi)]^n, & -\phi_1 < \phi < \phi_1, \\ 0, & \text{elsewhere}, \end{cases} \tag{5}$$

where P_{max} is the maximum load in the direction of the radial load, ε is the load distribution factor, $\pm\phi_1$ is the extent of load zone and $n = \frac{3}{2}$ for ball bearings and $\frac{10}{9}$ for roller bearings.

Since the load is periodic in nature, having a frequency equal to the cage frequency, and the load is evenly distributed about the point of maximum deflection, the ball/roller load can be expanded in Fourier series for even functions. Therefore, for a pure radial load

$$P(\omega_c t) = P_o + \sum_r P_r \cos r\omega_c t. \tag{6}$$

The Fourier coefficients P_o and P_r can be determined by the following method.

Since $(1 - \cos\phi)/2\varepsilon < 1$ for a non-zero load, $P(\phi)$ can be expanded in a binomial series,

$$P(\phi) = P_{max}[A_0 + A_1 \cos\phi + A_2 \cos 2\phi + A_3 \cos 3\phi], \tag{7}$$

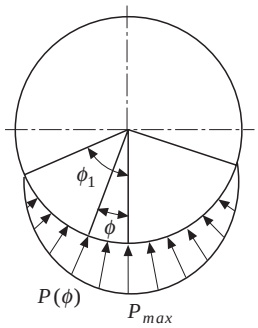

Figure 1. The load distribution in a bearing under radial load.

where

$$A_0 = 1 - \frac{n}{2\varepsilon} + \frac{n(n-1)}{8\varepsilon^2} \times \frac{3}{2} - \frac{n(n-1)(n-2)}{48\varepsilon^3} \times \frac{5}{2}, \tag{8a}$$

$$A_1 = \frac{n}{2\varepsilon} - \frac{n(n-1)}{8\varepsilon^2} \times 2 + \frac{n(n-1)(n-2)}{48\varepsilon^3} \times \frac{15}{4}, \tag{8b}$$

$$A_2 = \frac{n(n-1)}{8\varepsilon^2} \times \frac{1}{2} - \frac{n(n-1)(n-2)}{48\varepsilon^3} \times \frac{3}{2}, \tag{8c}$$

$$A_3 = \frac{n(n-1)(n-2)}{48\varepsilon^3} \times \frac{1}{4}. \tag{8d}$$

Therefore,

$$P_o = \frac{1}{T_c} \int_{-T_c/2}^{T_c/2} P(\omega_c t)\, \mathrm{d}t,$$

where T_c is the time period for cage motion $= 2\pi/\omega_c$,

$$P_o = \frac{P_{max}}{\pi} [A_0\phi_1 + A_1 \sin \phi_1 + (A_2/2) \sin 2\phi_1 + (A_3/3) \sin 3\phi_1], \tag{9}$$

$$P_r = \frac{2}{T_c} \int_{-T_c/2}^{T_c/2} P(\omega_c t) \cos r\omega_c t \, \mathrm{d}t$$

$$= \frac{P_{max}}{\pi} \left[\frac{2A_0}{r} \sin r\phi_1 + \sum_{l=1}^{3} A_l \left\{ \frac{\sin (r+l)\phi_1}{(r+l)} + \frac{\sin (r-l)\phi_1}{(r-l)} \right\} \right]. \tag{10}$$

2.2.2. *The pulse shape*

Because of its very short duration, there is a tendency to neglect the pulse width and to consider it an impulse. However, it has been pointed out in references [4, 8] that the severity, extent and age of the damage can be better represented by pulses. These factors certainly influence the amplitude of response. Therefore, in the present work, pulses of finite width have been considered. Since these pulses occur at regular time intervals, they are periodic in nature, and the frequency of occurrence depends on the location of the defect.

Some typical pulse forms are shown in Figure 2. In practice, the pulse forms may not be of such a regular shape as shown in the figure. The pulse width, ΔT, can be determined by dividing the defect width by the relative velocity between the mating elements [4]. The relative velocity, v_r, between the rolling element and either of the races, can be expressed as

$$v_r = \frac{D\omega_s}{4} \left(1 - \frac{d^2}{D^2} \cos^2 \alpha \right). \tag{11}$$

Therefore

$$\Delta T = b/v_r, \tag{12}$$

where b is the width of the defect.

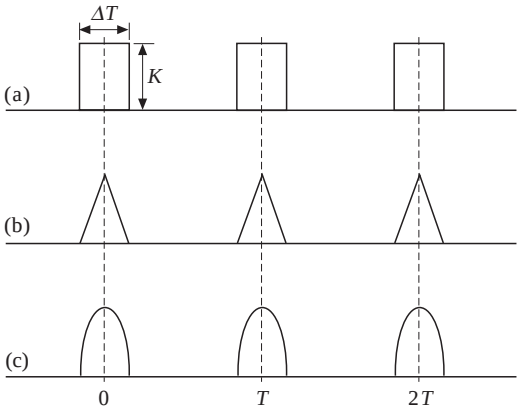

Figure 2. Different pulse forms: (a) rectangular; (b) triangular; (c) half-sine pulse.

The height of the pulse, K, also has a significant influence on the amplitude. This also changes with the severity and age of the defect and may even decrease with the advancement of the defect [8].

For simplicity, we assume these pulses to be even functions (Figure 2). Therefore they can be expanded in a Fourier series,

$$F(t) = F_o + \sum_s F_s \cos s\omega t, \tag{13}$$

where ω is the frequency of the generated pulses, which depends on the location of the defect. The Fourier coefficients, F_o and F_s, for different pulse forms are given in Appendix II.

2.2.3. *Mode shape*

The mode shape for the bearing ring can be assumed as

$$X_i(\phi) = \sin i\phi + \cos i\phi. \tag{14}$$

With the assumed mode shape, the generalized mass M_i for a bearing ring equals the actual mass of the ring. Therefore,

$$M_i = 2\pi\rho a. \tag{15}$$

3. SOLUTIONS FOR VARIOUS DEFECT LOCATIONS

Equations (2) and (3) are solved for the generalized co-ordinates, for different Q_i (or Q_i') derived for the various types of defects considered. The total deflection is obtained by multiplying each generalized co-ordinate by its mode shape and then linearly adding them for all of the modes.

3.1. OUTER RACE DEFECT

Since the outer race is assumed to be stationary, the rolling element load is a function of the angular position of the defect, which remains constant. Therefore, the generalized

force from equation (4) can be expressed as

$$Q_i = F(t) \int_0^{2\pi} P(\phi) X_i(\phi) \delta(\phi - \xi)\, \mathrm{d}\phi$$

$$= F(t) P(\xi) X_i(\xi). \tag{16}$$

The pulse $F(t)$ has a time period of $2\pi/\omega_c$. Therefore, the generalized force causing vibration of the outer race due to the impact of the kth rolling element can be expressed as

$$Q_i = P(\xi) X_i(\xi) \sum_s F_s \cos s(\omega_c t - \theta_k), \tag{17}$$

where $\theta_k = 2\pi\ k/Z$, Z being the total number of rolling elements in the bearing.

Q_i obtained from equation (17) is substituted into equation (2), which is then solved for the generalized co-ordinates. The deflection of the outer race due to the impact of the kth rolling element can be expressed as

$$y_k = \left(\sum_i \frac{P(\xi) X_i(\xi)}{M_i \omega_i^2} \right) \sum_s F_s \cos s(\omega_c t - \theta_k). \tag{18}$$

Therefore the deflection of the bearing ring due to the impact of all the rolling elements can be obtained by linearly adding the responses due to the impact of individual rolling elements. It is to be noted that summation over θ_k makes all terms in the summation over s equal to zero, except those for which s is a multiple of Z. Therefore, the total radial deflection is as follows:

$$y = \left(\sum_i \frac{P(\xi) X_i(\xi)}{M_i \omega_i^2} \right) \cdot \sum_s Z F_{Zs} \cos Zs\omega_c t\,. \tag{19}$$

Therefore, the frequency spectrum of the displacement for both radial and axial load will have components at $Zj\omega_c$ ($j = 1, 2, 3, \ldots$); i.e., the outer race defect frequency and its multiples. The amplitude of the component at $Zj\omega_c$ is

$$Y_{Zj\omega_c} = \left(\sum_i \frac{P(\xi) X_i(\xi)}{M_i \omega_i^2} \right) Z F_{Zj}. \tag{20}$$

For an axial load, $P(\xi)$ is constant for any position of the defect, but for a radial load, $P(\xi)$ changes with the change in position of the defect.

3.2. INNER RACE DEFECT

When a defect on the inner race is struck by the rolling elements, the response obtained is mainly due to the vibration of inner race. The relevant geometry is shown in Figure 3. The frequency of impact of a particular rolling element with a defect on the inner race is $(\omega_c - \omega_s)$.

Since the inner race is not stationary, the ball/roller load is a function of time. The

generalized force due to the impact of inner race defect with a rolling element is

$$Q_i' = P(\omega_c t)F(t)\int_0^{2\pi} X_i(\phi)\delta[\phi - (\omega_c - \omega_s)t]\,\mathrm{d}\phi$$

$$= P(\omega_c t)F(t)X_i[(\omega_c - \omega_s)t]. \tag{21}$$

The pulse $F(t)$ has a period of $2\pi/(\omega_c - \omega_s)$ and, therefore, $F(t)$ can be expressed as

$$F(t) = F_0 + \sum_s F_s \cos s(\omega_c - \omega_s)t. \tag{22}$$

3.2.1. *Axial loading*

In the case of axial loading, the generalized force due to the striking of the defect by the kth rolling element is

$$Q_i' = P_t F_o[\sin i(\omega_c t - \omega_s t - \theta_k) + \cos i(\omega_c t - \omega_s t - \theta_k)]$$

$$+ \sum_s \frac{P_t F_s}{2}[\sin (i+s)(\omega_c t - \omega_s t - \theta_k) + \sin (i-s)(\omega_c t - \omega_s t - \theta_k)$$

$$+ \cos (i+s)(\omega_c t - \omega_s t - \theta_k) + \cos (i-s)(\omega_c t - \omega_s t - \theta_k)]. \tag{23}$$

Substituting the sine and cosine terms of Q_i' from equation (23) into equation (3) and solving it, the generalized co-ordinates $q_{i,\sin}'$ and $q_{i,\cos}'$ can be obtained. While doing so, it has been considered that

$$\omega_i'^2 \gg i^2(\omega_c - \omega_s)^2, \quad (i \pm s)^2(\omega_c - \omega_s)^2.$$

Therefore, the response of the inner race due to the impact of the kth rolling element

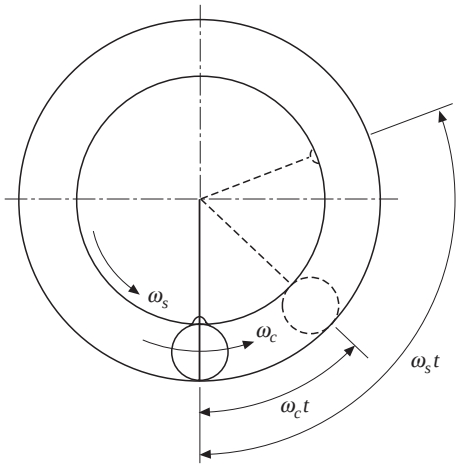

Figure 3. The bearing geometry for an inner race defect.

with the defect is

$$y'_k = \sum_i [q'_{i,\sin} \sin i\phi + q'_{i,\cos} \cos i\phi]$$

$$= \sum_i \frac{P_t F_o}{M'_i \omega'^2_i} \cos i[(\omega_c - \omega_s)t - \theta_k - \phi]$$

$$+ \sum_i \sum_s \frac{P_t F_s}{2M'_i \omega'^2_i} \cos [(i \pm s)(\omega_c t - \omega_s t - \theta_k) - i\phi]. \quad (24)$$

Therefore, the total deflection due to the impact of all the rolling elements can be obtained by adding all of the y_k linearly and taking care of the phase difference θ_k. Hence the deflection of the inner race can be expressed as

$$y' = \sum_i \frac{ZP_t F_o}{M'_{zi} \omega'^2_{zi}} \cos Zi[(\omega_c - \omega_s)t - \phi]$$

$$+ \sum_i \sum_s \frac{ZP_t F_s}{M'_i \omega'^2_i} \cos [(i \pm s)(\omega_c t - \omega_s t) - i\phi] \delta_T(Zj - i \pm n), \quad (25)$$

where δ_T is Kronecker delta function and $j = 1, 2, 3, \ldots$.

The frequency spectrum of the deflection will have components at $Zj(\omega_c - \omega_s)$; i.e., the inner race defect frequency and its harmonics. The amplitude of these components will be

$$Y_{Zj(\omega_c - \omega_s)} = \frac{ZP_t F_o}{M'_{Zj} \omega'^2_{Zj}} + \sum_s \frac{ZP_t F_s}{2M'_{Zj \pm s} \omega'^2_{Zj \pm s}}. \quad (26)$$

3.2.2. *Radial loading*

In the case of a bearing under pure radial load, the generalized force for the kth rolling element can be obtained from equation (21) as

$$Q'_i = \left[P_o + \sum_i P_r \cos r(\omega_c t - \theta_k) \right] \left[F_o + \sum_s F_s \cos s(\omega_c t - \omega_s t - \theta_k) \right]$$

$$\times X_i[(\omega_c - \omega_s)t - \theta_k]. \quad (27)$$

Following the same procedure as in the case of axial loading, the total radial deflection for the inner race can be obtained. The frequency spectrum of the deflection will have peaks at $Zj\ (\omega_c - \omega_s)$; i.e., inner race defect frequency and its multiples. The amplitude of these peaks will be

$$Y_{Zj(\omega_c - \omega_s)} = \frac{ZP_o F_o}{M'_{Zj} \omega'^2_{Zj}} + \sum_s \frac{ZP_o F_s}{2M'_{Zj \pm s} \omega'^2_{Zj \pm s}}. \quad (28)$$

In addition to these peaks, the spectrum will have sidebands at frequencies $Zj(\omega_c - \omega_s) \pm r\omega_s$; i.e., the sidebands will be at the shaft frequency and its multiples about

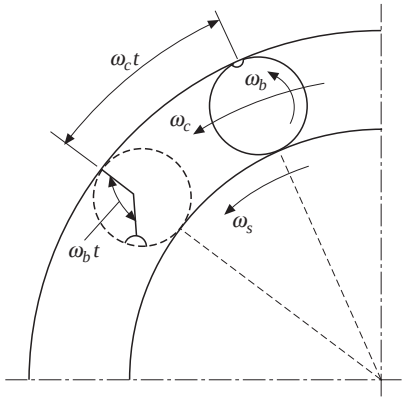

Figure 4. The bearing geometry for a rolling element defect.

the inner race defect frequency and its multiples. The amplitude of the sideband at $Zj(\omega_c - \omega_s) + r\omega_s$ will be

$$Y_{Zj(\omega_c - \omega_s) + r\omega_s} = \frac{ZP_rF_o}{2M'_{Zj-r}\omega'^2_{Zj-r}} + \sum_i \sum_s \frac{ZP_rF_s}{4M'_i\omega'^2_i}\,\delta_T[(Zj - r) - (i \pm s)]. \tag{29}$$

3.3. ROLLING ELEMENT DEFECT

The defect on the rolling element, which is spinning and revolving, strikes both the inner as well as the outer race (Figure 4). Therefore the resultant response is the sum of the deflections of the inner and outer races.

3.3.1. *Axial loading*

The generalized force for vibration of the outer race due to the rolling element defect is

$$Q_i = P_tF(t)X_i(\omega_b t) \tag{30}$$

The pulse $F(t)$ has a period of $2\pi/\omega_b$. Therefore,

$$F(t) = F_o + \sum_s F_s \cos s\omega_b t. \tag{31}$$

Substituting the value of Q_i from equation (30) into equation (2), we obtain the deflection of the outer race as

$$y = \sum_i \frac{P_tF_o}{M_i\omega_i^2} \cos i(\omega_b t - \phi)$$

$$+ \sum_i \sum_s \frac{P_tF_s}{2M_i\omega_i^2} \cos [(i \pm s)\omega_b t - i\phi]. \tag{32}$$

The defect on the rolling element makes an impact with the inner race at an interval of a half-time period ($=\pi/\omega_b$) after making an impact with the outer race. Therefore, the deflection of the inner race, y', has a phase difference of π with the deflection of outer race.

Therefore, the resultant response is

$$y_R = y + y'. \tag{33}$$

Thus, we obtain

$$y_R = \sum_i P_t \left(\frac{F_o}{M_{2i-1}\omega_{2i-1}^2} - \frac{F_o}{M'_{2i-1}\omega_{2i-1}^{\prime 2}} \right) \cos (2i-1)(\omega_b t - \phi)$$

$$+ \sum_i \sum_s \frac{P_t}{2} \left(\frac{F_s}{M_i \omega_i^2} - \frac{F_s}{M'_i \omega_i^{\prime 2}} \right) \cos [(i \pm s)\omega_b t - i\phi] \delta_T [(2j-1) - (i \pm s)]$$

$$+ \sum_i P_t \left(\frac{F_o}{M_{2i}\omega_{2i}^2} + \frac{F_o}{M'_{2i}\omega_{2i}^{\prime 2}} \right) \cos 2i(\omega_b t - \phi)$$

$$+ \sum_i \sum_s \frac{P_t}{2} \left(\frac{F_s}{M_i \omega_i^2} - \frac{F_s}{M'_i \omega_i^{\prime 2}} \right) \cos [(i \pm s)\omega_b t - i\phi] \delta_T [(2j - i \pm s), \tag{34}$$

where $j = 1, 2, 3, \ldots$.

Therefore, the frequency spectrum will have significant components at $2j\omega_b$; i.e., the rolling element defect frequency and its multiples. The amplitude of the component at $2j\omega_b$

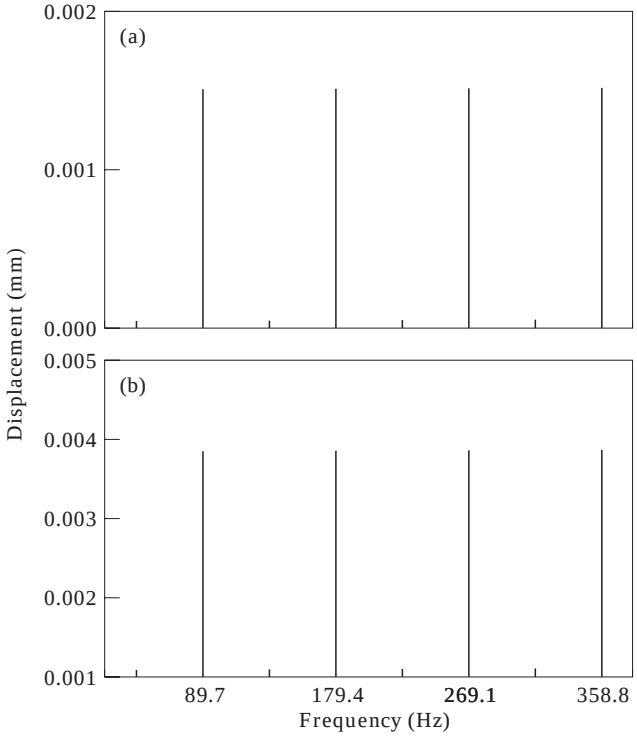

Figure 5. The frequency spectrum for an outer race defect at 10° and a radial load of (a) 20 kg and (b) 60 kg.

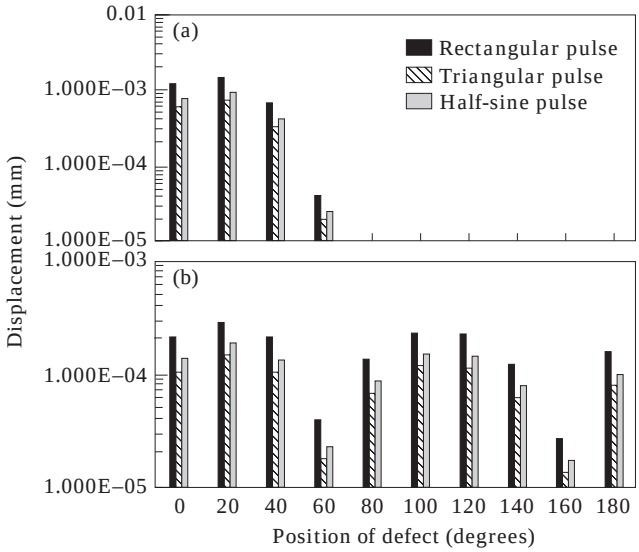

Figure 6. The variation in the amplitude for an outer race defect at different positions: (a) radial = 20 kg; (b) axial load = 20 kg.

is

$$Y_{2j\omega_b} = P_t\left(\frac{F_o}{M_{2j}\omega_{2j}^2} + \frac{F_o}{M'_{2j}\omega_{2j}'^2}\right) + \sum_s \frac{P_t}{2}\left(\frac{F_s}{M_{2j\pm s}\omega_{2j\pm s}^2} + \frac{F_s}{M'_{2j\pm s}\omega_{2j\pm s}'^2}\right). \tag{35}$$

In addition to these main components, there will be smaller components at ω_b and its odd multiples. However, these components will not have any significant presence in the frequency spectrum of vibration due to rolling element defects.

3.3.2. *Radial loading*

In the case of a bearing under pure radial load, the generalized force for the ith mode is

$$Q_i = P(\omega_c t)F(t)X_i(\omega_b t), \tag{36}$$

where $P(\omega_c t)$ and $F(t)$ are given by equations (6) and (31) respectively.

Following the same procedure as that adopted in case of axial loading, we can obtain the deflections of the outer and inner races, and by combining them the resultant response can be obtained.

The frequency spectrum for the resultant response will have main peaks at $2j\omega_b$, the harmonics of the rolling element defect frequency. The amplitude of the component at $2j\omega_b$ is

$$Y_{2j\omega_b} = P_o\left[\frac{F_o}{M_{2j}\omega_{2j}^2} + \frac{F_o}{M'_{2j}\omega_{2j}'^2}\right] + \sum_s \frac{P_o}{2}\left[\frac{F_s}{M_{2j\pm s}\omega_{2j\pm s}^2} + \frac{F_s}{M'_{2j\pm s}\omega_{2j\pm s}'^2}\right]. \tag{37}$$

In addition to these peaks, there will be sidebands at the cage frequency and its multiples ($r\omega_c$) about the rolling element defect frequency and its multiples ($2j\omega_b$). The amplitude

of the sideband at $2j\omega_b \pm r\omega_c$ will be

$$Y_{2j\omega_b \pm r\omega_c} = \frac{P_r}{2}\left[\frac{F_o}{M_{2j}\omega_{2j}^2} + \frac{F_o}{M'_{2j}\omega'^2_{2j}}\right] + \sum_s \frac{P_r}{2}\left[\frac{F_s}{M_{2j\pm s}\omega_{2j\pm s}^2} + \frac{F_s}{M'_{2j\pm s}\omega'^2_{2j\pm s}}\right]. \tag{38}$$

4. RESULTS AND DISCUSSION

A 6002 deep groove ball bearing with normal clearance has been considered for obtaining numerical results for the expressions for the frequencies and amplitudes obtained in section 3. The dimensions of the 6002 ball bearing are as follows: 15 mm bore, 32 mm outside diameter, 9 mm width, 4·76 mm ball diameter and 23·5 mm pitch diameter. The groove radii for the inner and outer races are 2·43 mm and 2·57 mm respectively. They have nine balls and the nominal contact angle is 0°. In the case of axial loading the contact angle should be 5–15°, but for simplicity a contact angle of 0° has been assumed. A spindle speed of 1500 rpm has been considered, and the value of the pulse height, K, has been assumed to be 1.

For the bearing geometry and spindle speed as mentioned above, the significant frequency components (as shown in Appendix I) are the shaft rotation frequency, 25 Hz, the cage frequency, 9·968 Hz, the outer race defect frequency, 89·7 Hz, the inner race defect frequency, 135·2 Hz, and the ball defect frequency, 118·3 Hz.

With the help of the above-mentioned dimensions of a bearing having steel races, the natural frequencies and generalized masses of the races for different modes can be obtained

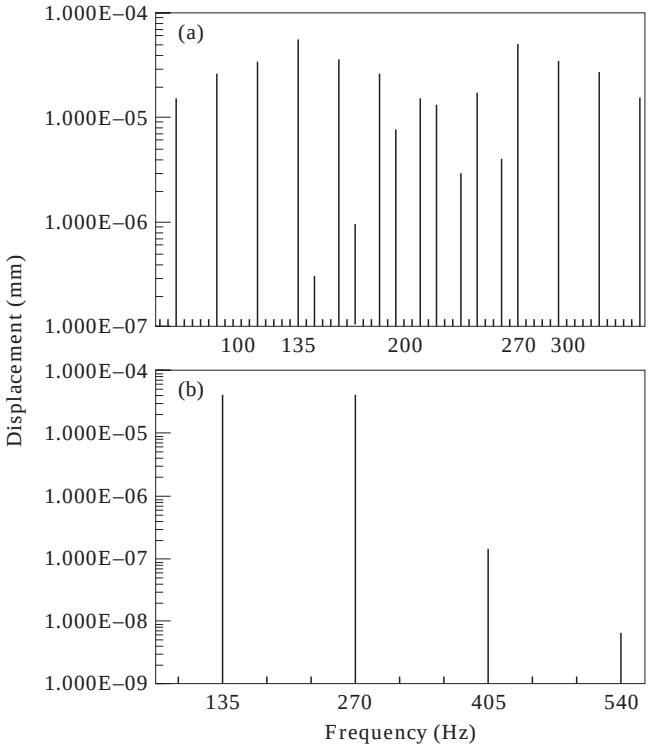

Figure 7. The frequency spectrum for an inner race defect causing a rectangular pulse: (a) radial load = 20 kg; (b) axial load = 20 kg.

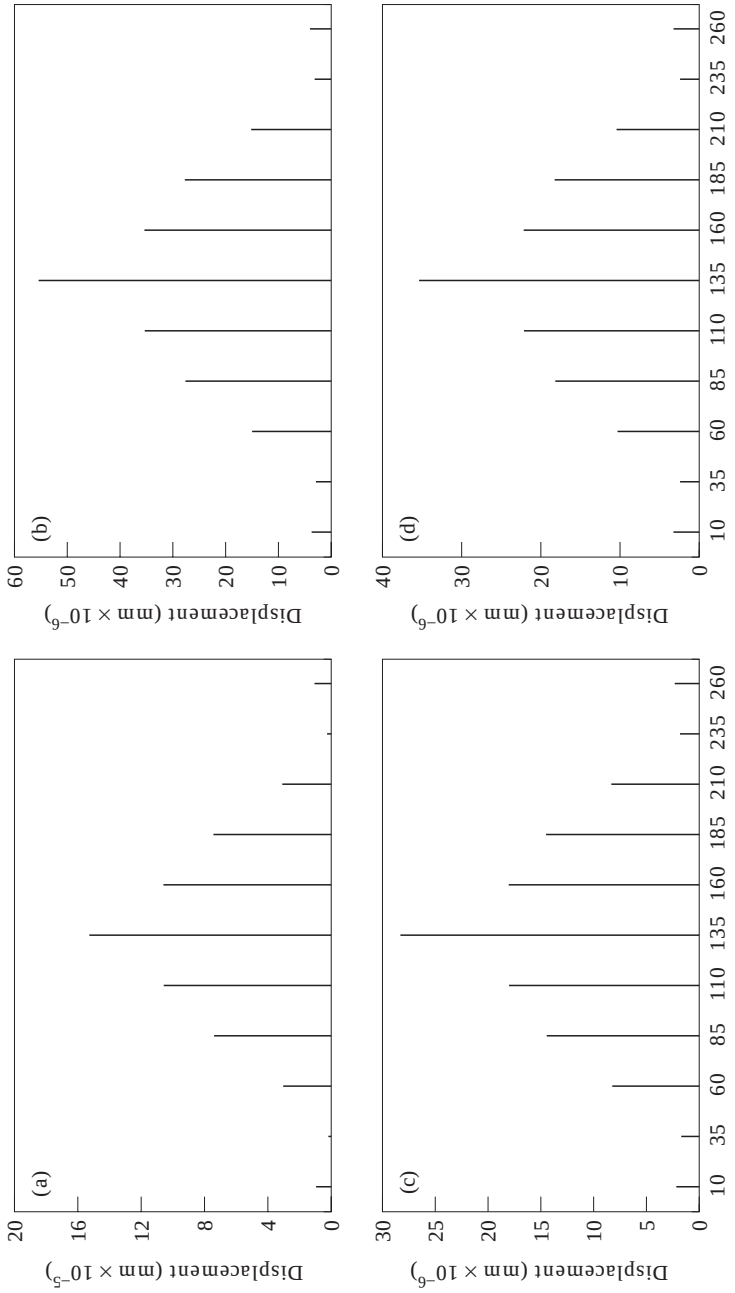

Figure 8. The effects of the load and the pulse shape for an inner race defect under a radial load: (a) rectangular pulse, 60 kg load; (b) rectangular pulse, 20 kg load; (c) triangular pulse, 20 kg load; (d) half-sine pulse, 20 kg load.

from equations (1) and (15) respectively. For this purpose, the bearing rings are assumed to have a rectangular cross-section, with grooves cut out of them, and the neutral surface is assumed to lie at the centre of the races. The values of P_o and P_r for different radial loads can be obtained from equations (9) and (10), respectively, by substituting the values of P_{max} and ϕ_1, which can be found following the procedure laid down in reference [7]. The values of P_t can also be obtained from the method given in reference [7]. The Fourier coefficients for the generated pulses, F_o and F_s can be determined using the expressions given in Appendix II, and a defect width of 150 μm has been considered to obtain these values. A computer program has been developed to determine the values of these parameters following the procedures mentioned above. The program also considers substitution of these values in equations (20), (26), (28), (29), (35), (37) and (38) to obtain the amplitudes of displacement for vibration generated due to defects on various bearing elements. These values are then plotted.

In Figures 5(a) and 5(b) it is shown that, for the outer race defect, there is a significant increase in the amplitude level with the increase in load. In Figure 6(a) it is shown that there is a large variation in amplitude for various positions of outer race defect under radial load. However, in Figure 6(b) it is shown that the variation is small for an axial load. This is due to the fact that in the case of a radial load, the amplitude is affected by the load as well as the mode shape, whereas in the case of an axial load, the amplitude will be affected by the mode shape only for different positions of the defect. The variation in amplitude due to the different pulse forms generated is also shown in Figures 6(a) and 6(b). The amplitude is a maximum at a 20° defect position because the contribution of the mode shape is a maximum at that position.

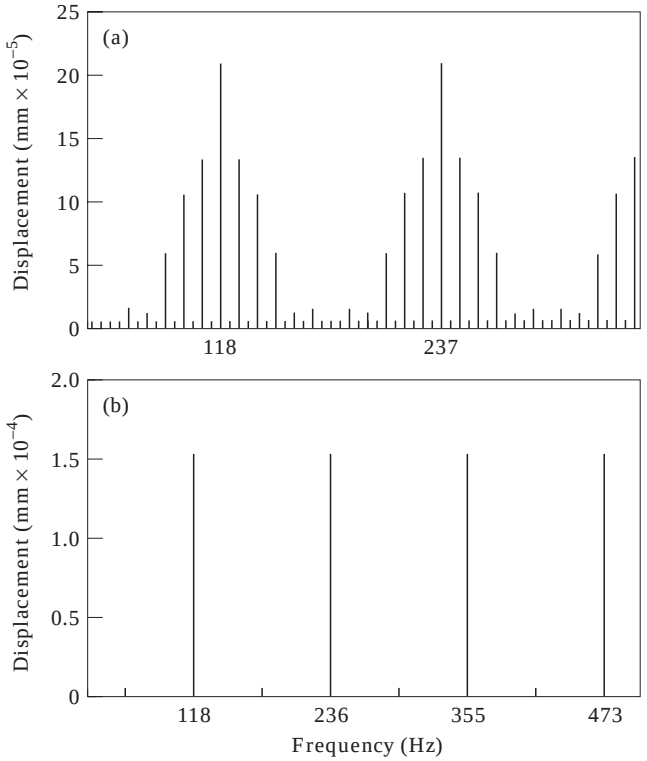

Figure 9. The frequency spectrum for a rolling element defect causing a rectangular pulse: (a) radial load = 20 kg; (b) axial load = 20 kg.

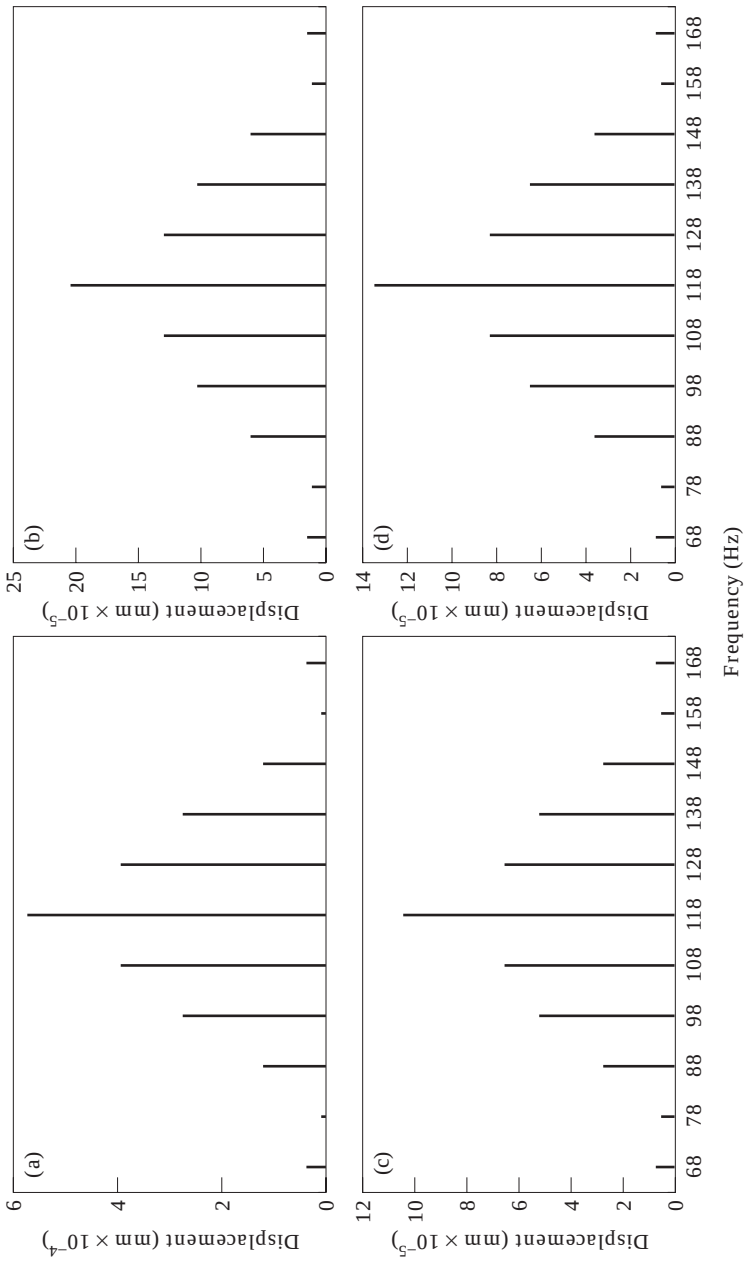

Figure 10. The effects of the load and the pulse shape for a rolling element defect under a radial load: (a) rectangular pulse, 60 kg load; (b) rectangular pulse, 20 kg load; (c) triangular pulse, 20 kg load; (d) half-sine pulse, 20 kg load.

In Figures 7(a) and 7(b) it is shown that the amplitude of the deflection at the inner race defect frequency and its second harmonics remains the same. However, the drop in amplitude in Figure 7(b) for higher harmonics may be due to failure of the analysis for the higher modes. In Figure 7(a) it is shown that the sidebands are evenly distributed about the main peak at the defect frequency.

In Figures 8(a) and 8(b) it is shown that with an increase in the load there is a significant increase in the amplitude of vibration and a decrease in the peak to sideband ratio. In Figures 8(b), (c) and (d) it is shown that there is a wide variation in the amplitude for different shapes of pulses having the same width and height.

In Figures 9(a) and 9(b) are shown the amplitudes of the responses for a rolling element defect frequency and its higher harmonies, in the case of radial and axial loads. In the case of a radial load, the sidebands occur symmetrically about the main peaks. In Figures 10(a)–(d) it is shown that the effect of the load and the pulse shape in the case of a rolling element defect under a radial load are similar to those for inner race defect.

It has been observed that the amplitude of the response for the outer race defect is much higher than those for other defects. Similar observations were also made in reference [9] about the overall r.m.s. level of acceleration obtained experimentally from a similar bearing. One of the reasons for this may be the fact that the natural frequencies of the outer race are smaller than the corresponding natural frequencies of the inner race.

The prediction of absolute amplitudes of vibration due to bearing defects will not be possible using this model, because that procedure has to take into account the effects of the total rotor–bearing system, including those of the shaft and the housing. However, the results of this analysis can be used to assess the approximate amplitude ratios among various spectral lines.

For this purpose, a comparison of the analytical values of the velocity amplitudes with the experimental values obtained from reference [9] for vibration generated due to the inner race defect (1·5 mm wide under a 60 kg radial load at 1500 rpm) is shown in Figure 11. The analytical values of the velocity amplitudes, determined by multiplying the displacement amplitudes by the corresponding frequencies, have been normalized with respect to the experimental value of the amplitude at the inner race defect frequency (135 Hz). The figure shows fair agreement between the analytical and experimental values. However, this comparison is restricted to the components at the inner race defect frequency and the sidebands about this component at multiples of the shaft frequency. Other significant components of the experimental spectrum [9], especially the peaks at the multiples of the shaft frequency, could not be predicted by this model.

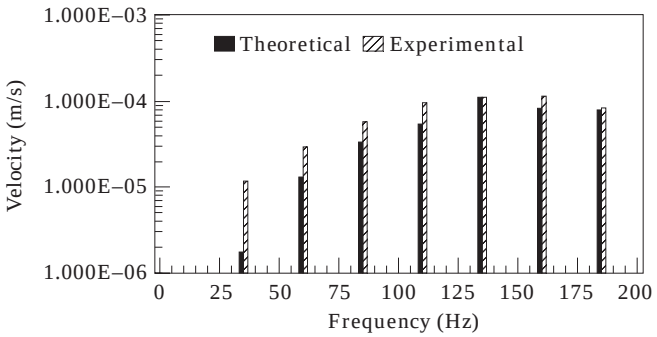

Figure 11. A comparison of analytical values of velocity amplitudes for an inner race defect with experimental values [9]: defect width = 1·5 mm, radial load = 60 kg, speed = 1500 rpm (analytical values normalized with respect to the experimental value at 135 Hz).

5. CONCLUSIONS

The model presented here predicts a frequency spectrum having peaks at characteristic defect frequencies with modulations in the case of a rolling element defect and an inner race defect under a radial load. The amplitudes at these frequencies are also predicted for various defect locations. The amplitude for the outer race defect is found to be quite high in comparison to those for the inner race defect and the rolling element defect. The amplitude level is also found to increase with an increase in load; and it is affected by the shapes of the generated pulses.

REFERENCES

1. C. S. Sunnersjo 1978 *Journal of Sound and Vibration* **58**, 363–373. Varying compliance vibrations of rolling bearings.
2. L. D. Meyer, F. F. Ahlgren and B. Weichbrodt 1980 *Transactions of the American Society of Mechanical Engineers*, *Journal of Mechanical Design* **102**, 205–210. An analytic model for ball bearing vibrations to predict vibration response to distributed defects.
3. N. Tandon and B. C. Nakra 1992 *The Shock and Vibration Digest* **24**, 3–11. Vibration and acoustic monitoring techniques for the detection of defects in rolling element bearings—a review.
4. T. Igarashi and H. Hamada 1982 *Bulletin of the Japan Society of Mechanical Engineers* **25**, 994–1001. Studies on the vibration and sound of defective rolling bearings (first report: vibration of ball bearings with one defect).
5. S. Timoshenko, D. H. Young and W. Weaver, Jr. 1974 *Vibration Problems in Engineering*. New York: John Wiley.
6. W. T. Thomson 1982 *Theory of Vibration with Applications*. New Delhi: Prentice-Hall of India.
7. T. A. Harris 1966 *Rolling Bearings Analysis*. New York: John Wiley.
8. M. F. White 1984 *Journal of Sound and Vibration* **93**, 95–116. Simulation and analysis of machinery fault signals.
9. N. Tandon and B. C. Nakra 1993 *Journal of the Institution of Engineers* (*India*)—*Mechanical Engineering Division* **73**, 271–282. Detection of defects in rolling element bearings by vibration monitoring.

APPENDIX I

For a bearing with a stationary outer race,

$$\text{cage frequency, } \omega_c(\text{rad/s}) = \frac{\omega_s}{2}\left(1 - \frac{d}{D}\cos\alpha\right),$$

$$\text{ball spinning frequency, } \omega_b(\text{rad/s}) = \frac{D\omega_s}{2d}\left[1 - \frac{d^2}{D^2}\cos^2\alpha\right],$$

$$\text{inner race defect frequency, } \omega_{id}(\text{rad/s}) = Z(\omega_s - \omega_c) = \frac{Z\omega_s}{2}\left(1 + \frac{d}{D}\cos\alpha\right),$$

$$\text{outer race defect frequency, } \omega_{od}(\text{rad/s}) = Z\omega_c = \frac{Z\omega_s}{2}\left(1 - \frac{d}{D}\cos\alpha\right),$$

$$\text{ball defect frequency, } \omega_{bd}(\text{rad/s}) = 2\omega_b = \omega_s\frac{D}{d}\left(1 - \frac{d^2}{D^2}\cos^2\alpha\right),$$

where ω_s is the shaft rotation frequency in rad/s, d is the ball diameter, D is the pitch diameter, Z is the number of rolling elements and α is the contact angle.

APPENDIX II: FOURIER COEFFICIENTS

For rectangular pulses (Figure 2(a)),

$$F(t) = \begin{cases} K, & -\dfrac{\Delta T}{2} < t < \dfrac{\Delta T}{2}, \\ 0, & \text{otherwise} \end{cases}$$

$$F_o = \frac{1}{T}\int_{-\Delta T/2}^{\Delta T/2} K \, \mathrm{d}t$$

$$= Km,$$

where

$$m = \Delta T/T,$$

$$F_s = \frac{4}{T}\int_{0}^{\Delta T/2} K \cos s\omega t \, \mathrm{d}t$$

$$= \frac{2K}{\pi s} \sin \pi s m.$$

For triangular pulses (Figures 2(b)),

$$F_o = Km/2, \qquad F_s = (2K/\pi^2 s^2 m)(1 - \cos \pi s m).$$

For half-sine pulses (Figure 2(c)),

$$F_o = 2Km/\pi, \qquad F_s = [4Km/\pi(1 - 4s^2 m^2)] \cos (\pi s m).$$